LETTERS

An aluminium nitride light-emitting diode with a wavelength of 210 nanometres

Yoshitaka Taniyasu[1], Makoto Kasu[1] & Toshiki Makimoto[1]

Compact high-efficiency ultraviolet solid-state light sources[1]—such as light-emitting diodes (LEDs) and laser diodes—are of considerable technological interest as alternatives to large, toxic, low-efficiency gas lasers and mercury lamps. Microelectronic fabrication technologies and the environmental sciences both require light sources with shorter emission wavelengths: the former for improved resolution in photolithography and the latter for sensors that can detect minute hazardous particles. In addition, ultraviolet solid-state light sources are also attracting attention for potential applications in high-density optical data storage, biomedical research, water and air purification, and sterilization. Wide-bandgap materials, such as diamond[2] and III–V nitride semiconductors (GaN, AlGaN and AlN; refs 3–10), are potential materials for ultraviolet LEDs and laser diodes, but suffer from difficulties in controlling electrical conduction. Here we report the successful control of both n-type and p-type doping in aluminium nitride (AlN), which has a very wide direct bandgap[11] of 6 eV. This doping strategy allows us to develop an AlN PIN (p-type/intrinsic/n-type) homojunction LED with an emission wavelength of 210 nm, which is the shortest reported to date for any kind of LED. The emission is attributed to an exciton transition, and represents an important step towards achieving exciton-related light-emitting devices as well as replacing gas light sources with solid-state light sources.

Recently, we have achieved n-type conduction in Si-doped AlN (refs 12, 13). In the present work, by reducing the dislocation density and finely controlling the Si doping level, we were able to boost the room-temperature electron mobility. We examined (by Hall-effect measurement) the temperature dependence of the electron concentration (n) and electron mobility (μ_n) for n-type Si-doped AlN with a Si doping concentration of $3.5 \times 10^{17}\,cm^{-3}$. At 300 K, the electron concentration was $7.3 \times 10^{14}\,cm^{-3}$. The electron mobility was $426\,cm^2\,V^{-1}\,s^{-1}$, which is the highest reported to date in n-type AlN and attests to the high quality of the AlN. As the temperature increased, the electron concentration increased exponentially and saturated at higher temperatures (Fig. 1a). The temperature dependence of electron concentration was fitted by the least-squares method, assuming the charge neutrality equation for n-type semiconductor with a shallow donor and a deep compensating acceptor[12]. The best-fit values are donor concentration $N_D = 3.0 \times 10^{17}\,cm^{-3}$, acceptor concentration $N_A = 2.6 \times 10^{16}\,cm^{-3}$ and donor ionization energy $E_D = 282$ meV. The donor concentration agreed well with the Si doping concentration, indicating that almost all Si atoms act as donors in AlN. The compensation ratio N_A/N_D was about 0.1. On the other hand, the electron mobility increased monotonically as temperature decreased (Fig. 1b). At 220 K, the electron mobility reached $730\,cm^2\,V^{-1}\,s^{-1}$. In calculating mobility, we took into account scattering by neutral impurities, ionized impurities, polar optical phonons, acoustic deformation potential, and piezoelectric potential[13]. We assumed Matthiesen's rule, and used the best-fit values of N_D, N_A and E_D, and the material parameters in ref. 13. The calculated electron mobility (solid line) agreed very well with the measured one. For n-type AlN with a higher dislocation density, the measured electron mobility was much smaller than the calculated one owing to the influence of scattering caused by charged dislocations[14] or unidentified dislocation-related defects. Thus, the agreement indicates that the quality of the n-type AlN layer is high.

With this success in achieving n-type conduction, we turned our attention to p-type conduction and found that Mg doping produced p-type AlN. The p-type conduction in Mg-doped AlN was observed at Mg doping concentrations below $2 \times 10^{20}\,cm^{-3}$. When the Mg doping concentration exceeded an upper limit of $2 \times 10^{20}\,cm^{-3}$, the Mg-doped AlN became highly resistive. This is similar to the tendency observed in n-type Si-doped AlN (ref. 12), and probably results from a self-compensation effect of Mg in p-type AlN. This indicates that control of the Mg doping concentration is important for obtaining p-type conduction. In addition, the as-grown Mg-doped AlN was highly resistive, and became p-type conductive after thermal annealing in N_2 at 800 °C for 10 min. For the highly resistive as-grown Mg-doped AlN, the H concentration was in the same range as the Mg concentration, and after annealing the H concentration decreased. This means that, in the as-grown AlN, H passivated Mg dopant, but after annealing H was desorbed and Mg was activated, as in GaN (ref. 15).

We measured the temperature dependence of hole concentration (p) and hole mobility (μ_p) for Mg-doped AlN with a Mg doping concentration of $2 \times 10^{19}\,cm^{-3}$. We clearly confirmed p-type conduction from the polarity of the Hall voltage, although there is some scattering of measured values because of the high resistivity (low

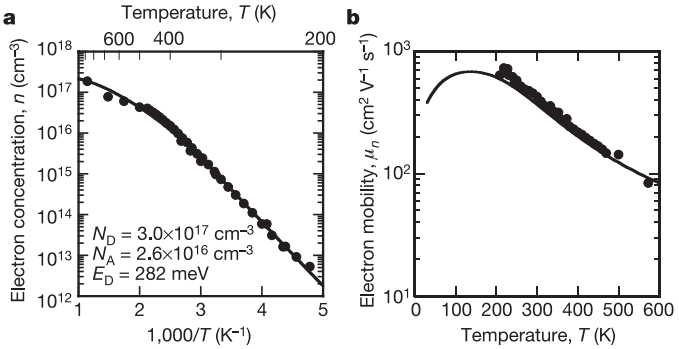

Figure 1 | Electrical characteristics of n-type Si-doped AlN. a, The temperature dependence of electron concentration. The solid line shows the least-squares fit, assuming the charge neutrality equation with a shallow donor and a deep compensating acceptor. The best-fit parameters are shown. **b**, The temperature dependence of electron mobility. The solid line shows the calculated mobility, considering specific scattering mechanisms (see text).

[1]NTT Basic Research Laboratories, NTT Corporation, 3-1 Morinosato-Wakamiya, Atsugi, 243-0198, Japan.

mobility). As the measurement temperature increased, the hole concentration increased exponentially (Fig. 2a). Accurately determining the acceptor concentration and compensating donor concentration in the p-type AlN would require fitting of the measured data in the high-temperature (exhausted) regime. Thus, from the present data, only the acceptor ionization energy E_A was obtained, by assuming that the hole concentration follows $\exp(-E_A/k_BT)$, where k_B is the Boltzmann constant and T is the sample temperature. The E_A was estimated to be 630 meV, which is in good agreement with an optically obtained value (510 meV)[16] and with a theoretically obtained value (465–758 meV)[17]. Owing to the high acceptor ionization energy, the room-temperature hole concentration is as low as of the order of $10^{10}\,cm^{-3}$. On the other hand, the hole mobility decreased as temperature increased (Fig. 2b). The temperature dependence was well fitted to $\mu \propto T^{-1.5}$ (broken line). This is typical of phonon scattering, which has the strongest influence on mobility in semiconductors at high temperature. To calculate the hole mobility, we used a method similar to the above-mentioned one for the electron mobility. In the calculation, we used the hole effective mass of AlN, $m_h^* = 3.3$, which we estimated from the acceptor ionization energy $E_A = 630$ meV and the effective mass theory. We assumed the Mg doping concentration of $2 \times 10^{19}\,cm^{-3}$ as the acceptor concentration, and the compensation ratio of p-type AlN, $N_D/N_A = 0.1$. This ratio was the same as that of the n-type AlN. Although the experimental mobility was slightly smaller than the calculated one (solid line), both showed a similar tendency. These results also support p-type conduction in the Mg-doped AlN.

The achievement of n-type and p-type AlN allowed us to make a p-type AlN/intrinsic (undoped) AlN/n-type PIN AlN LED (Fig. 3a). The LED consists of an AlN PIN homojunction sandwiched between a p-type and an n-type AlN/AlGaN superlattice[18]. The superlattices were used to improve the lateral conduction in the n-type region and reduce the contact resistance of the electrodes, and thereby lower the driving voltage of the LED. The average carrier concentration of the superlattices is as high as $10^{18}\,cm^{-3}$, because the doping efficiency of the superlattices is much higher than that of the AlN layers. The high doping efficiency originates both from the large band offset between AlN and AlGaN layers and from large band bending caused by strong polarization fields in the superlattices. A metal/undoped AlN (insulator)/n-type AlN (semiconductor) MIS LED was also fabricated to clarify the conduction and emission mechanisms of the LEDs (Fig. 3b).

The characterization of the electrical and optical properties was performed on-wafer under a direct current (d.c.) bias condition at room temperature. The current–voltage (I–V) characteristics of both LEDs showed rectifying properties, with rectification ratios of higher than 10^4 at ±40 V (Fig. 3c). The current increased remarkably above voltages V_D of 5 V for the PIN LED and 3.8 V for the MIS LED. These voltages are close to the diffusion (built-in) potential of the PIN and MIS junctions. Below V_D, the current was as low as <0.1 μA. This low current is probably due to lower energy barriers at the metal/AlN interface and the n-type AlN/n-type superlattice interface. Above V_D, the current is limited by a high series resistance, which originates from the p-type and undoped AlN layers. Consequently, the operating voltages at 20 mA were about 45 V and 37 V for the PIN and MIS LEDs, respectively, and were much higher than the voltages estimated from the diffusion potentials. The operating voltage of the PIN LED is higher than that of the MIS LED because of a voltage drop in the p-type AlN as well as that in the undoped AlN.

For the PIN LED, the electroluminescence spectra were observed at a wavelength of approximately 210 nm (Fig. 3d). This emission wavelength was almost the same as that of the free-exciton recombination of an undoped AlN layer measured by photoluminescence at room temperature (Fig. 3e). We also assigned the excitonic structure of our AlN layer by cathodoluminescence and photoreflectance. The excitons in AlN are stable even at room temperature ($k_BT = 26$ meV) because of the large exciton binding energy of 80 meV (ref. 11). This indicates that the origin of the electroluminescence is unambiguously

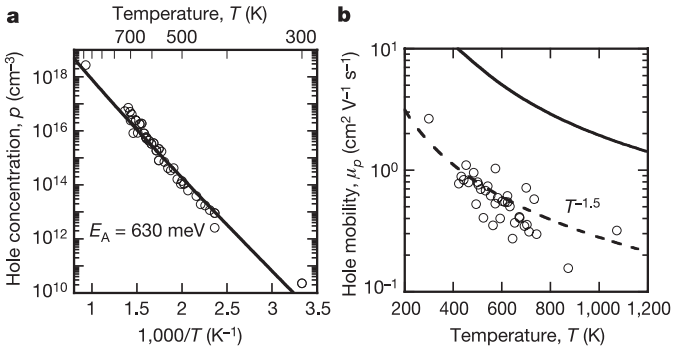

Figure 2 | Electrical characteristics of p-type Mg-doped AlN. **a**, The temperature dependence of hole concentration. The solid line shows the least-squares fit by $\exp(-E_A/k_BT)$, where E_A is the acceptor ionization energy, k_B the Boltzmann constant, and T the sample temperature. The best-fit parameter is shown. **b**, The temperature dependence of hole mobility. The broken line is a least-squares fit of data with $\mu \propto T^{-1.5}$. The solid line shows the calculated mobility, assuming the hole effective mass m_h^* of 3.3, the acceptor concentration N_A of $2 \times 10^{19}\,cm^{-3}$, and the compensation ratio N_D/N_A of 0.1.

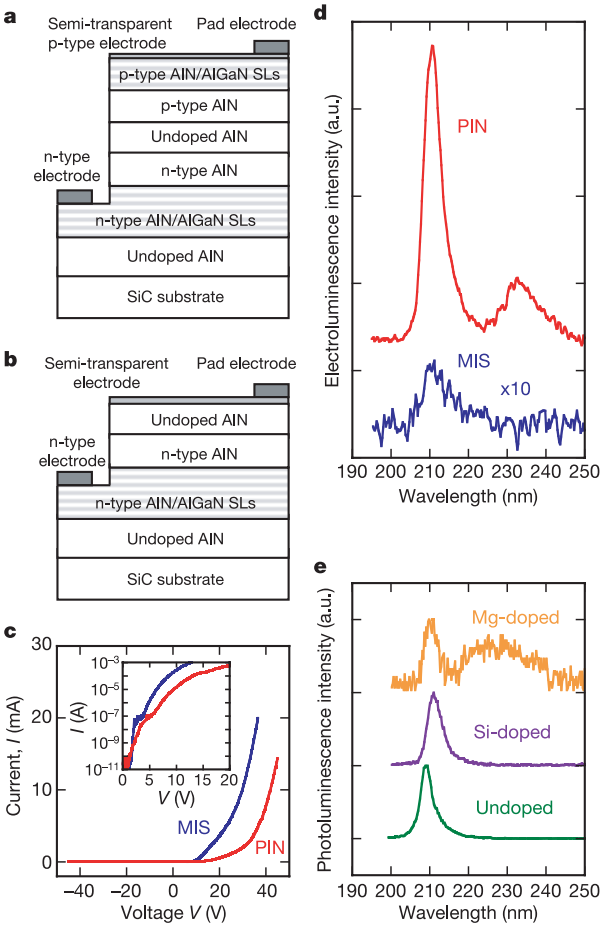

Figure 3 | AlN LEDs. **a**, Schematic illustration of the PIN LED. **b**, Schematic illustration of the MIS LED. **c**, Current–voltage (I–V) characteristics of the LEDs under a d.c. bias condition. The inset is plotted on a semilogarithmic scale. **d**, Electroluminescence spectra of the LEDs under a d.c. bias condition. **e**, Photoluminescence spectra of undoped, Si-doped and Mg-doped AlN. Data in **c**–**e** were measured at room temperature. a.u., arbitrary units; see text for explanation of PIN and MIS.

the near-band-edge recombination in the AlN. The electroluminescence intensity increased with current. As the current increased from 10 mA to 40 mA, the emission wavelength slightly shifted from 209 nm to 210 nm. This is because of a self-heating effect, which results from the relatively high operating voltage. From the temperature dependence of the free-exciton recombination energy[19], the increase of junction temperature ΔT was estimated to be about 60 °C at 40 mA. In addition to the near-band-edge emission, a weak emission attributed to the Mg impurity level in the p-type AlN layer was observed at around 230 nm. On the other hand, a broad emission peak attributed to the Si impurity level in n-type AlN was also observed at around 400 nm.

We now discuss the conduction and emission mechanisms in the LEDs. For the MIS LED, emission at 210 nm was also observed. This indicates that holes are injected from the electrode by tunnelling and then recombine radiatively with electrons injected from the n-type AlN. The emission intensity of the PIN LED is more than 70 times as high as that of the MIS LED. This confirms that, for the PIN LED, p-type AlN and p-type superlattices improve the emission efficiency, and that the most of holes are injected from the p-type layers. On the other hand, the series resistance, $R_S = dV/dI$, was 10^6–$10^5\,\Omega$ at 6–10 V. The R_S is almost the same as a resistance of $5 \times 10^5\,\Omega$ for hole transport in the p-type AlN, which was calculated from the result of the Hall-effect measurement. These indicate that, at low voltages, the diffusion and tunnelling processes are dominant in the conduction mechanism.

The value of R_S decreased with voltage. At high voltages of around 40 V, R_S decreased to about 500 Ω and has a linear relation with the inverse of current for both PIN and MIS LEDs. Such characteristics are commonly observed in PIN diodes operated under a high-voltage condition at which drift current limits the conduction[20]. In our PIN LED, because the hole concentration in the p-type AlN is still low, only a few of the injected electrons recombine radiatively with the injected holes around the undoped AlN, while most of the electrons injected from the n-type AlN overflow through the undoped AlN to the p-type AlN and then to the p-type electrode. The Mg-related emission in electroluminescence supports this electron overflow. Therefore, at high voltage, electron drift current becomes dominant in the conduction mechanism. As a result, R_S is determined by the injected electron transport in the undoped and p-type AlN, and becomes smaller than that determined by the hole transport in the p-type AlN.

The output power of the near-band-edge emission at wavelength $\lambda = 210$ nm was measured to be about 0.02 μW at a d.c. current of 40 mA. The external quantum efficiency η_{ext} of our on-wafer device was estimated to be of the order of 10^{-6}%, which is still lower than that for typical packaged commercial visible LEDs ($\eta_{ext} \approx 10\%$). The external quantum efficiency is given by the product of the extraction efficiency η_{out} and the internal quantum efficiency η_{in}, that is, $\eta_{ext} = \eta_{out} \times \eta_{in}$. The estimated η_{out} and η_{in} are of the order of 10^{-1}% and 10^{-3}%, respectively. The reason for the low η_{out} is that emitted light is absorbed by the SiC substrate, the AlN/AlGaN superlattices, and the p-type metal contact in the device. The η_{out} would be increased by using transparent substrates and proper packaging, and by optimizing the device structure.

However, increasing internal quantum efficiency η_{in} is much more important at this stage. Possible approaches to improving η_{in} effectively are to decrease dislocation density, introduce carrier confinement structures, and increase the p-type doping efficiency; we now consider these options in turn. First, our device still has a high dislocation density of $10^9\,cm^{-2}$ as a result of the lattice mismatch and the heterovalency between the SiC substrate and the AlN layer. For AlN layers, in a dislocation-density range of 10^9–$10^{10}\,cm^{-2}$, the photoluminescence intensities, which are related to η_{in}, linearly increased with decreasing dislocation density. Thus, the dislocations act as non-radiative recombination centres. It has also been reported for LEDs made with other nitride semiconductors that the output power increased by a factor of about 10^3 with decreasing dislocation density from 10^{11} to $10^7\,cm^{-2}$ (ref. 21). The use of AlN substrate[22], which has a low dislocation density of $10^4\,cm^{-2}$, will decrease the dislocation density in the device and thereby increase the η_{in} by a factor of 10^2. Second, η_{in} generally increases by about 10^2 times by introducing carrier confinement structures (double heterostructures or quantum well structures), which are normally used for practical devices. BN in the zinc blende structure is an indirect bandgap material. The indirect (Γ–X transition) and direct (Γ–Γ transition) bandgap energies are 6.4 eV and about 8 eV, respectively[23], which are wider than AlN's direct bandgap. Therefore, BN or AlBN can confine carriers in the AlN active layer. Third, increasing the hole concentration in p-type AlN will enhance η_{in} because the hole concentration injected into the AlN active layer will increase. We have used Mg for p-type dopant, which is commonly used for nitride semiconductors, but Mg's doping efficiency in AlN is quite low. Alternative elements for the acceptor with lower ionization energy need to be explored—group II or IV elements (Be, Zn, Cd, or C) are potential candidates.

METHODS

Device manufacture. The layer structure of the AlN PIN LED (Fig. 3a) was grown on SiC(0001) substrate by low-pressure metal organic vapour phase epitaxy. The sources were trimethylaluminium, trimethylgallium and ammonia (NH_3). For n-type and p-type doping, Si and Mg atoms were doped by introducing silane (SiH_4) and bis-cyclopentadienylmagnesium (Cp_2Mg) during growth, respectively. We decreased the dislocation density to $2 \times 10^9\,cm^{-2}$ by suppressing the parasitic reaction of the sources (trimethylaluminium and NH_3) in the gas phase during the growth. The details of the growth procedure have been reported elsewhere[12,13]. The PIN LED consisted of a 750-nm-thick undoped AlN layer, n-type uniformly Si-doped 100-period AlN/AlGaN (1.2 nm/3 nm) superlattices with a Si doping concentration [Si] of $3 \times 10^{19}\,cm^{-3}$, a 200-nm-thick n-type Si-doped AlN layer with [Si] of $2 \times 10^{18}\,cm^{-3}$, a 60-nm-thick undoped (insulating) AlN layer, a 20-nm-thick p-type Mg-doped AlN layer with a Mg doping concentration [Mg] of $4 \times 10^{19}\,cm^{-3}$, and p-type uniformly Mg-doped three-period AlN/AlGaN (1.2 nm/3 nm) superlattices with [Mg] of $4 \times 10^{19}\,cm^{-3}$. The structure of the MIS LED (Fig. 3b) is the same as that of the PIN LED except for the p-type AlN and p-type superlattices. A mesa structure 200 μm × 200 μm in size was formed by dry etching with Cl_2 gas down to the n-type superlattices. An n-type Ti/Al/Ti/Au (25/100/50/100 nm) electrode was formed on the n-type superlattices, while a semi-transparent (transparency $T \approx 50\%$ at $\lambda = 210$ nm) p-type Pd/Au (2.5/1.5 nm) electrode was formed on the p-type superlattices for the PIN LED and on the undoped AlN for the MIS LED. A pad electrode was then evaporated on the Pd/Au electrode.

Measurements. The mobility and carrier concentration were obtained by Hall-effect measurement in the Van der Pauw configuration. For the Hall-effect measurement of highly resistive (low mobility) samples, we applied an a.c. magnetic field to improve the signal-to-noise ratio. The electroluminescence spectra of the LED at various d.c. currents were measured with a monochromator equipped with a ultraviolet-enhanced charge coupled device array. The output power of the electroluminescence was measured with a Si photodiode located above the device. The output power of the near-band-edge emission was obtained by taking the intensity ratio between the near-band-edge emission and impurity-related emission into account.

Received 8 November 2005; accepted 24 March 2006.

1. Schubert, E. F. & Kim, J. K. Solid-state light sources getting smart. *Science* **308,** 1274–1278 (2005).
2. Koizumi, S., Watanabe, K., Hasegawa, M. & Kanda, H. Ultraviolet emission from a diamond p-n junction. *Science* **292,** 1899–1901 (2001).
3. Akasaki, I. & Amano, H. Crystal growth and conductivity control of group III nitride semiconductors and their application to short wavelength light emitters. *Jpn. J. Appl. Phys.* **36,** 5393–5408 (1997).
4. Pankove, J. I., Miller, E. A., Richman, D. & Berkeyheiser, J. E. Electroluminescence in GaN. *J. Lumin.* **4,** 63–66 (1971).
5. Nakamura, S. *et al.* Superbright green InGaN SQW structure LEDs. *Jpn. J. Appl. Phys.* **34,** L1332–L1335 (1995).
6. Ponce, F. A. & Bour, D. P. Nitride-based semiconductors for blue and green light-emitting devices. *Nature* **386,** 351–359 (1997).
7. Han, J. *et al.* AlGaN/GaN quantum well ultraviolet light emitting diodes. *Appl. Phys. Lett.* **73,** 1688–1690 (1998).

8. Nishida, T. & Kobayashi, N. 346 nm emission from AlGaN multi-quantum-well light emitting diode. *Phys. Status Solidi A* **176,** 45–48 (1999).
9. Adivarahan, V. *et al.* 250 nm AlGaN light-emitting diodes. *Appl. Phys. Lett.* **85,** 2175–2177 (2004).
10. Hirayama, H. Quaternary InAlGaN-based high efficiency ultraviolet light-emitting diodes. *J. Appl. Phys.* **97,** 091101 (2005).
11. Li, J. *et al.* Band structure and fundamental optical transitions in wurtzite AlN. *Appl. Phys. Lett.* **83,** 5163–5165 (2003).
12. Taniyasu, Y., Kasu, M. & Kobayashi, N. Intentional control of n-type conduction for Si-doped AlN and $Al_xGa_{1-x}N$ ($0.42 \leq x < 1$). *Appl. Phys. Lett.* **81,** 1255–1257 (2002).
13. Taniyasu, Y., Kasu, M. & Makimoto, T. Electrical conduction properties of n-type Si-doped AlN with high electron mobility ($>100\,cm^2\,V^{-1}\,s^{-1}$). *Appl. Phys. Lett.* **85,** 4672–4674 (2004).
14. Ng, H. M. *et al.* The role of dislocation scattering in n-type GaN films. *Appl. Phys. Lett.* **73,** 821–823 (1998).
15. Nakamura, S., Mukai, T., Senoh, M. & Iwasa, N. Thermal annealing effects on p-type Mg-doped GaN films. *Jpn. J. Appl. Phys.* **31,** L139–L142 (1992).
16. Nam, K. B. *et al.* Mg acceptor level in AlN probed by deep ultraviolet photoluminescence. *Appl. Phys. Lett.* **83,** 878–880 (2003).
17. Mireles, F. & Ulloa, S. E. Acceptor binding energies in GaN and AlN. *Phys. Rev. B* **58,** 3879–3887 (1998).
18. Taniyasu, Y., Kasu, M., Kumakura, K., Makimoto, T. & Kobayashi, N. High electron concentrations in Si-doped AlN/AlGaN superlattices with high average Al content of 80%. *Phys. Status Solidi A* **200,** 40–43 (2003).
19. Kuokstis, E. *et al.* Near-band-edge photoluminescence of wurtzite-type AlN. *Appl. Phys. Lett.* **81,** 2755–2757 (2002).
20. Sze, S. M. *Physics of Semiconductor Devices* 2nd edn 63–132 (Wiley, New York, 1981).
21. Amano, H. *et al.* Defect and stress control of AlGaN for fabrication of high performance UV light emitters. *Phys. Status Solidi A* **201,** 2679–2685 (2001).
22. Rojo, J. C. *et al.* Report on the growth of bulk aluminium nitride and subsequent substrate preparation. *J. Cryst. Growth* **231,** 317–321 (2001).
23. Edgar, J. H. *Properties of Group III Nitrides* 129–134 (INSPEC, London, 1994).

Acknowledgements We thank M. Prinz, K. Thonke and R. Sauer at the University of Ulm in Germany for measurement of free-exciton energy in our AlN by cathodoluminescence and photoreflectance. We are also grateful to K. Kumakura for discussions, and K. Torimitsu and H. Takayanagi for their encouragement.

Author Contributions Y.T. performed experimental work and data analysis. All authors discussed results.

Author Information Reprints and permissions information is available at npg.nature.com/reprintsandpermissions. The authors declare no competing financial interests. Correspondence and requests for materials should be addressed to Y.T. (taniyasu@will.brl.ntt.co.jp).